JOURNAL OF MATERIALS SCIENCE 30 (1995) 63–68

The effects of boundary conditions on the basal glide of ice crystals in compression

P. D. BARRETTE, N. K. SINHA
Institute for Environmental Research and Technology, National Research Council, Building M-17, Ottawa, Canada K1A OR6

E. STANDER, B. MICHEL
Dépt Génie Civil, Université Laval, Ste-Foy, Qc, Canada G1K 7P4

Creep experiments were conducted on ice crystals in compression to investigate the effects of boundary conditions on a single-slip system deformed in plane strain. Friction at the platens of the deformation apparatus introduces a bending moment which causes a variation in the amount of lattice rotation across the specimen. This is shown to occur in mechanically constrained crystals observed through plane polarized light. Relieving the constraints and minimizing friction at the ice-platen contact leads to the widening of the sample near the specimen–platen interface and the production of 'tails' symmetrically disposed about the longitudinal axis of the deformed crystals. This is interpreted to originate from a bending moment in the opposite sense from that obtained in the constrained crystals, resulting from a progressive increase in slip displacement towards the platens where the segments of the slip plane become shorter. When the crystal ends were constrained but allowed to move sideways, a simple shear regime was established in which lattice slip was concentrated in the centre of the crystal.

1. Introduction

Plasticity describes the behaviour of a crystalline solid as it achieves permanent deformation. It is the macroscopic expression of processes involving the generation and mobilization of lattice defects along slip systems whose nature depends on the crystallographic structure of the material [1]. This type of deformation is evidenced by changes in length and rotation of material lines resulting from their displacement by slip [2]. It does not affect either volume or lattice parameters.

Fig. 1 illustrates the simplest case of an ideal single-slip system subjected to a compression regime, where slip occurs along the projection of the applied stress onto the slip plane. A passive marker in the form of a rectangular outline, corresponding to a given material element, undergoes shear along planes oriented at a given angle with respect to the compression axis. As deformation proceeds, both sets of parallel faces will remain so but the angle that they make with each other will diverge increasingly from 90°. This change in geometry occurs in no other plane than that which comprises the load direction and the pole to the active slip plane. It is referred to as plane strain deformation.

The material element shown in Fig. 1 to behave as a passive marker may also be represented as a specimen deformed in a compression apparatus. There are, however, inherent difficulties when attempting to physically reproduce this simulation. Most importantly, the application of the load must conform to the change in shape of the specimen. Two set-ups may be envisaged (Fig. 2). In the first, the upper and lower surfaces are allowed to rotate by means of a universal joint while the side surfaces remain parallel to the load direction (Fig. 2b). This alternative is merely conceptual as it would lead in practice, if at all possible, to a dangerously unstable condition, as both joints need to be perfectly aligned throughout the deformation in a plane containing the stress direction. Such a design is more suitable for a tensional load system.

In the second set-up (Fig. 2c), the upper and lower surfaces are maintained parallel to the platens while shifting sideways with respect to each other to accommodate internal shear. In doing so, the slip planes rotate away from the direction of compression about an axis normal to the plane of the paper (as shown in Fig. 1). This scheme's major limitation is that it requires perfect lubrication at the specimen–platen contacts, a condition which is difficult to achieve. The high stresses involved in the deformation of most material require a method of keeping the lubricant from being expelled from this interface [3]. In creep tests, most lubricant will either evaporate or react with the deforming material at the temperature at which the test is being conducted [4, 5]. When friction is high and the platens remain parallel, uniaxial compression translates into a bending moment which, in turn, leads to a heterogeneous internal strain distribution [6–8] (Fig. 2d).

Ice is defined as a hydrogen-bonded assemblage of water molecules [9]. Its most common form belongs to the hexagonal system and has a c/a lattice ratio of

0022–2461

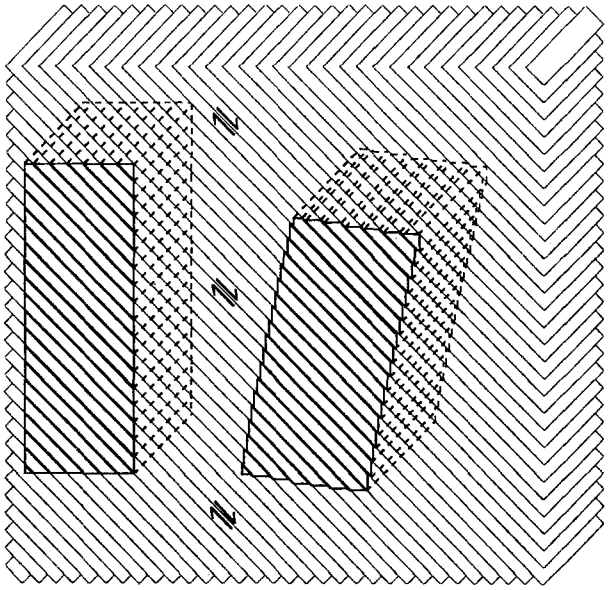

Figure 1 Three-dimensional representation of an ideal single-slip system in plane strain. A rectangular block acts as a passive marker enclosed in a series of 'stacked' surfaces (left). When these surfaces are made to slip upon each other (right), the block assumes a new shape in which all material lines initially oriented at an angle to the slip planes will have rotated. Shear strain is 0.35.

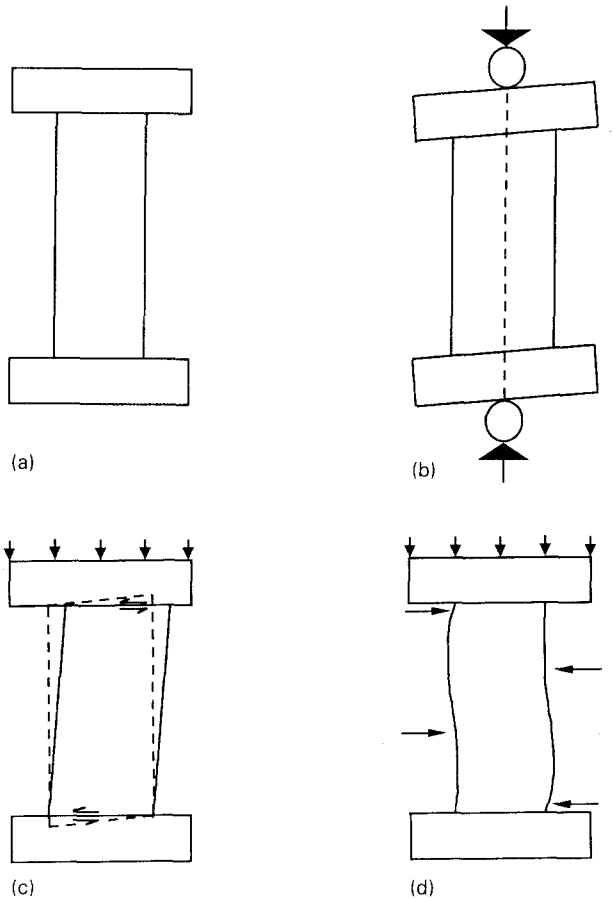

Figure 2 The simulation depicted in Fig. 1 will be successfully reproduced providing the change in shape of the sample (shown in the undeformed state in (a)) is accommodated by the platens of the deformation apparatus in either of two ways: (1) by allowing the rotation of the platens about an axis perpendicular to the plane of the paper (b); or (2) by ensuring perfect lubrication at the platen–specimen interface (c). Failure to do so will result in unequal load distribution (as inferred from the dashed outline in (c), representing the shape of the crystal shown in (b)) and a departure from a uniaxial state of stress, thereby inducing plastic bending (d).

1.628 [9, 10]. Although eleven slip systems have been identified [11], dislocation slip occurs predominantly on the basal (0 0 0 1) plane [12, 13], reported as the only easy glide plane in ice [14–17]. Non-basal linear lattice defects contribute to plastic strain insofar as they constitute a source of dislocation multiplication on that plane [13, 18]. Burger's vectors are $a_0/3$ $[1\,1\,\bar{2}\,0]$, $a_0/3$ $[\bar{2}\,1\,1\,0]$ and $a_0/3$ $[1\,\bar{2}\,1\,0]$ which, combined, lead to isotropic slip [10, 19].

Ice is well suited to the investigation of a material dominated by single-slip in a near frictionless environment. It creeps at temperatures well within the range at which most hydrocarbon-based lubricants are effective. The normalized stress in a given test, defined as the ratio of the applied stress over the elastic moduli, is significantly lower (typically by a factor of 20) on the hardware used in the experimental set-up than it is on the ice specimen. Furthermore, ice is transparent and birefringent. Sections of the entire specimen may be prepared in which the internal structure may be readily observed through cross-polarized light [20].

This paper discusses the influence of boundary conditions on the geometrical evolution of ice single crystals undergoing primarily basal creep in compression, with a focus on the interaction between the anvils of the deformation apparatus and the single-slip system of the material.

2. Materials and methods

The ice specimens used in this study were obtained by the repetitive seeding of singly distilled deaerated water with an ice platelet comprising one large, optically continuous crystal of known orientation [21]. The resulting sheet was cut with a band saw into rectangular prisms which were then shaved with a microtome blade, to sizes of $40 \times 40 \times 90$ mm or $40 \times 40 \times 110$ mm $\pm$ 1 mm.

Crystallographic orientation was monitored with a universal stage [22] and a chemical etching technique, the latter according to principles described previously [23]. The [0 0 0 1] axis of the crystal specimens used in this study was at an angle of 30 and 45° $\pm$ 3° to the load direction and a $\langle 1\,1\,\bar{2}\,0 \rangle$ axis in the plane comprising the load direction and the [0 0 0 1] axis. Procedures for surface preparation and etching were those of Sinha [24, 25], which allowed line defect characterization of the crystals after loading. All specimens were enclosed in a thin sheet of cellophane during deformation to prevent sublimation.

The compression apparatus was of the dead-load type, and designed so that the surface of the upper platen remained parallel to that of the lower while moving downward (as shown in Fig. 2c, d). A 3-mm thick sheet of rubber was inserted between the ice and the platens to avoid localized stress concentration. The stress applied on all samples was in the range 300–500 kPa at a temperature of -2 ± 0.5 °C (corresponding to an homologous temperature of $0.993T_m$, where T_m is the melting point in (K)).

3. Boundary conditions

Three types of boundary conditions were investigated (Fig. 3). The restriction mode R was designed to

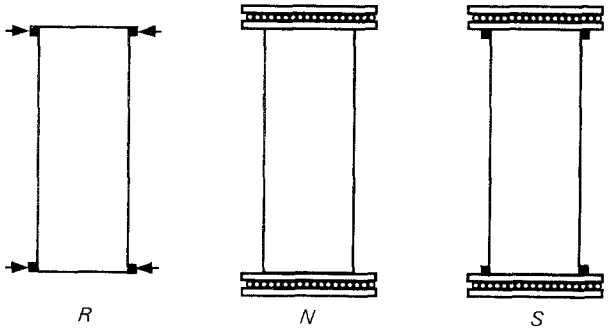

Figure 3 Three types of boundary conditions. (See text for discussion.)

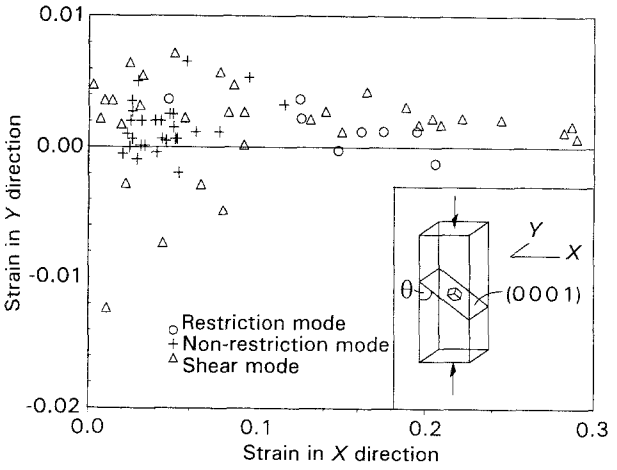

Figure 4 Linear plot displaying the relationship between the axial strain in the X and Y directions of ice crystals deformed under uniaxial compression. The angle θ for all samples is 45°. (See text for discussion.)

simulate high friction experiments. The upper and lower surfaces were held at a constant width with aluminium prismatic rods (filled squares in Fig. 3). These were, in turn, attached to the frame of the press with threaded steel wires (represented by arrows) so as to prevent those surfaces from moving sideways with respect to each other.

The non-restriction mode N, on the other hand, was meant to reproduce uniaxial deformation experiments in which the interface between the material and the platens was as close to frictionless as possible. It was found in early experiments that ice adherence to the platens was minimal. However, to ensure that the specimen was allowed to widen *and* shift freely sideways, a sheet of steel ball-bearings 2.3 mm in diameter, held together in lithium grease and sandwiched between two 3-mm thick tempered steel platelets, was inserted at both ends of the specimen. In some cases, either Teflon tape or lithium grease was added between the specimen's wrapping and the steel platelet, with similar results.

The shear mode S is a combination of the two previous modes. Aluminium rods prevented the ends of the specimens from widening, but they were able to move sideways with respect to each other with the steel platelets and ball-bearings assemblages.

Wielding of the specimen onto the surface of the platens did not hold at the temperature at which the experiments were conducted. However, this technique proved effective in one test run at $-12\,^{\circ}C$ ($T/T_m = 0.956$) but it is uncertain as to how much additional restriction it added to that already imposed by the aluminium rods.

4. Results and interpretation

The lateral strain of six specimens, corresponding to the variation in width over total width, was measured at various sites across their length (Fig. 4). The results indicate that deformation approximated plane strain. Data scattering at the low end of the X scale is attributed to the lateral restraint imposed near the platens by the R and S mode boundary conditions. In general, this promoted extension in the Y direction. The four lowest data points on the Y scale are from one specimen that may have been inadequately protected against sublimation during storage.

4.1. Restriction mode

Bending activates a reversal in shear stress gradient on opposite sides of the bending plane which mobilizes dislocations of one sign into polygonization or tilt walls [8] (Fig. 5). These reflect the internal strain distribution expressed by the mobilization of linear lattice defects into a low energy configuration [8, 26, 27]. It occurs concurrently with a spatial variation in lattice orientation. Dislocations of the other sign eventually reach the external surfaces of the specimen, thereby contributing to its change in shape.

All ice crystals having crept under R mode boundary conditions displayed a slightly asymmetric 'barrel shape' configuration and two paired sets of subgrain boundaries symmetrically disposed about the centre of the specimen (Fig. 6). The latter are interpreted as tilt walls [28].

4.2. Non-restriction mode

Specimens deformed under the N mode boundary conditions displayed a distinctly non-uniform shear strain gradient. Widening of the crystals was significantly higher at their ends than in the centre (Figs 7, 8). This is particularly evident in specimens with the (0 0 0 1) plane initially oriented at 60° to the direction of loading, where 'tails' developed in two opposite corners (Fig. 7).

This feature is best interpreted as an artefact of sample geometry. As deformation proceeds, dislocations are generated and move towards one of the specimen's surfaces. Those on the shorter segments of the basal plane, located closest to two of the four corners of the specimen, should reach one of these surfaces first. Hence, for a given amount of internal shear, the displacement due to slip will increase towards the platens in these areas (Fig. 9). In this process, the slip planes rotate towards the upper and lower surfaces at a rate exceeding that expected if shear strain was uniformly distributed in the specimen. This is the reverse situation to that obtained under R mode boundary conditions, where such rota-

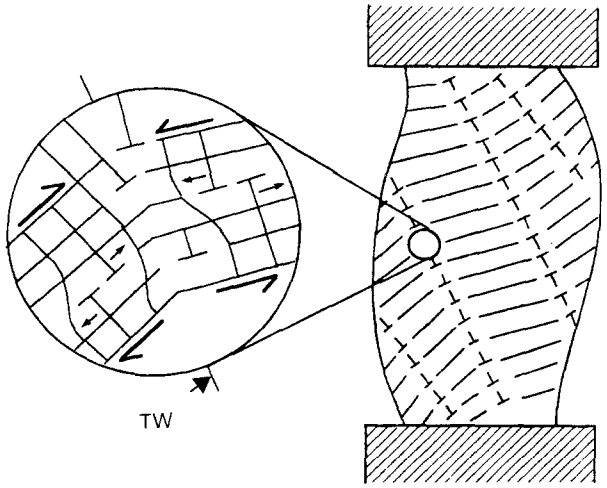

Figure 5 Dislocation distribution in a material specimen deforming by single slip under compression, whose ends are constrained at the platens (adapted from [8]). TW: tilt wall. (See text for discussion.)

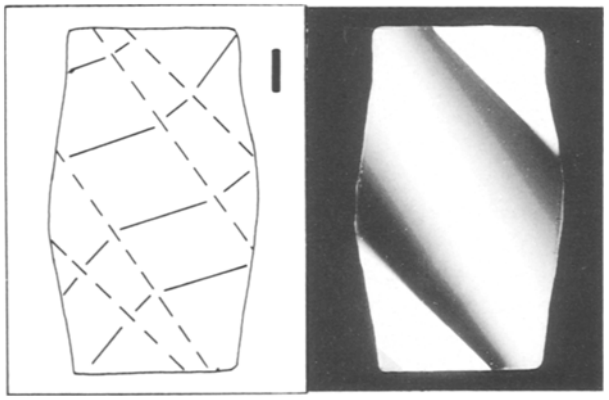

Figure 6 Section, 3.5 mm in thickness (viewed under cross-polarized light), of a single crystal deformed to 10% axial strain under *R* mode boundary conditions. The trace of the (0 0 0 1) plane, initially oriented at 45° to the load axis, is represented by a full line. Tilt walls are indicated by dashed lines and separate areas of different illumination. Length of the scale bar: 10 mm.

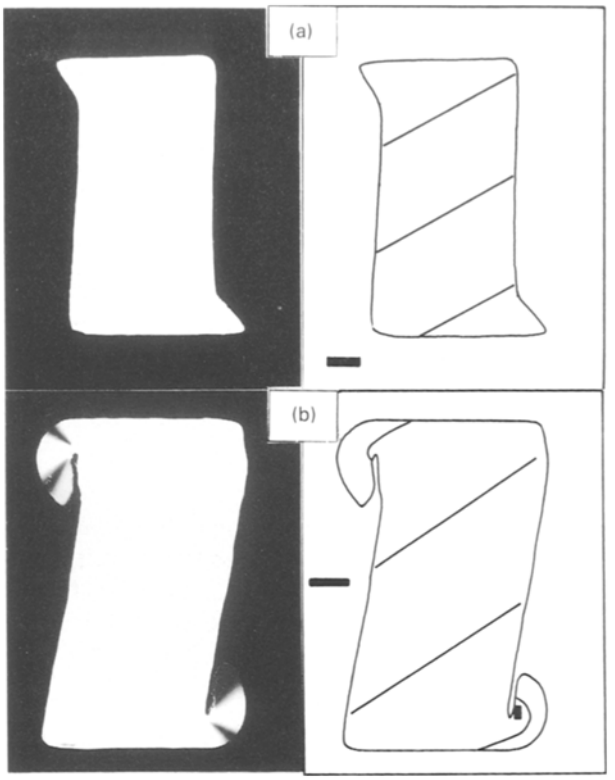

Figure 7 Two examples of strained crystals with (0 0 0 1) plane initially oriented at 60° to the load axis, deformed under *N* mode boundary conditions. Axial strain in (a) is 8% and (b) 17%. Viewed under crossed polars. The sections are 5.5 and 10.4 mm in thickness, respectively. Filled rectangle in (b): location of Fig. 10. Full lines represent the trace of the (0 0 0 1) plane. Length scale bars: 10 mm.

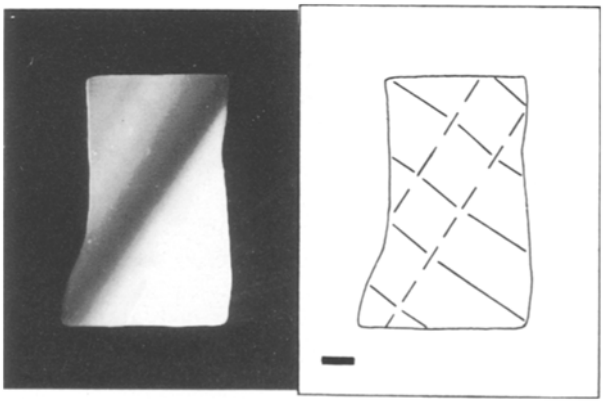

Figure 8 Crystal with its (0 0 0 1) plane initially oriented at 45° to the load axis deformed to 21% axial strain under *N* mode boundary conditions (viewed under crossed polars). The section is 4.5 mm in thickness. Full lines represent the trace of the (0 0 0 1) plane. Dashed lines are zones of change in the crystallographic orientation within the crystal. Length of scale bar: 10 mm.

tion is impeded near the platens. A bending moment of opposite sense is thus transmitted to the specimen.

In 45° crystals, this leads to a spatial variation in the slope of the (0 0 0 1) plane which follows a course opposite to that observed in the constrained crystals: it is steeper in the centre and shallower near the platens (compare Figs 6 and 8). Dislocations accumulate along tilt walls in the centre of the specimen and are thus prevented from reaching one of the free surfaces. In 60° crystals, such tilt walls are short and confined to the corners of the specimen where the tail develops (Fig. 10). 'Folding in' of the tails with increasing strain in these crystals is interpreted to result from inhomogeneous slip, as shown in Fig. 9, followed by the local accumulation of edge dislocations of one sign (Fig. 11).

4.3. Shear mode

By keeping the upper and lower surfaces of the crystal from widening, slip along lattice planes intersecting these surfaces and the resulting variation in the amount of lattice rotation are considerably reduced, as seen also under *R* mode boundary conditions. By allowing the areas of limited slip, represented by two triangular zones, to shift sideways, they acted as rigid blocks or 'dummies' (Fig. 12). Upon compression, these subjected the central part of the specimen to a simple shear regime not unlike that obtained in other studies with a shear box or Bausch's apparatus

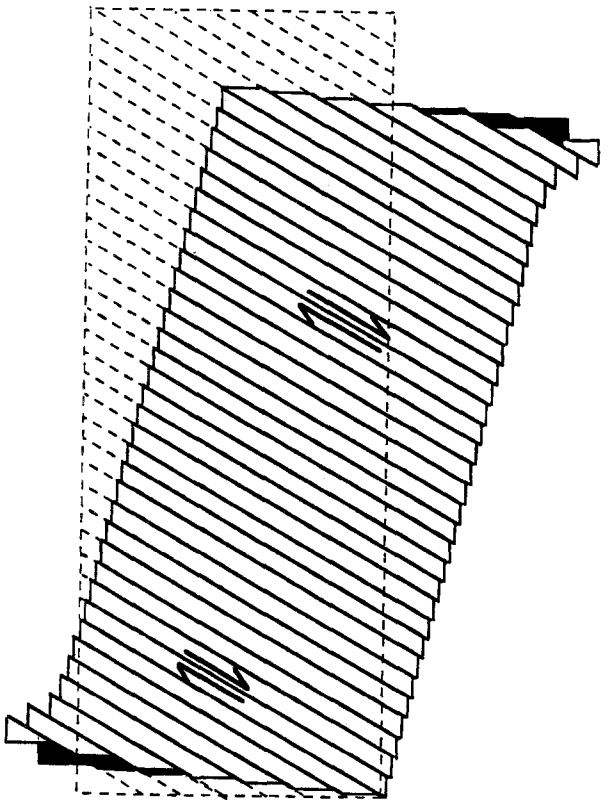

Figure 9 Simulation of a single-slip system under compression, assuming arbitrarily that the amount of slip displacement due to shear is linearly proportional to the length of the lattice plane along which the displacement takes place. The amount of shear in the centre of the crystal is 0.28 and increases to an average of 0.67 near the platens. The dark areas outline the shape of the crystal if shear strain had been uniform (as for the case shown in Fig. 1).

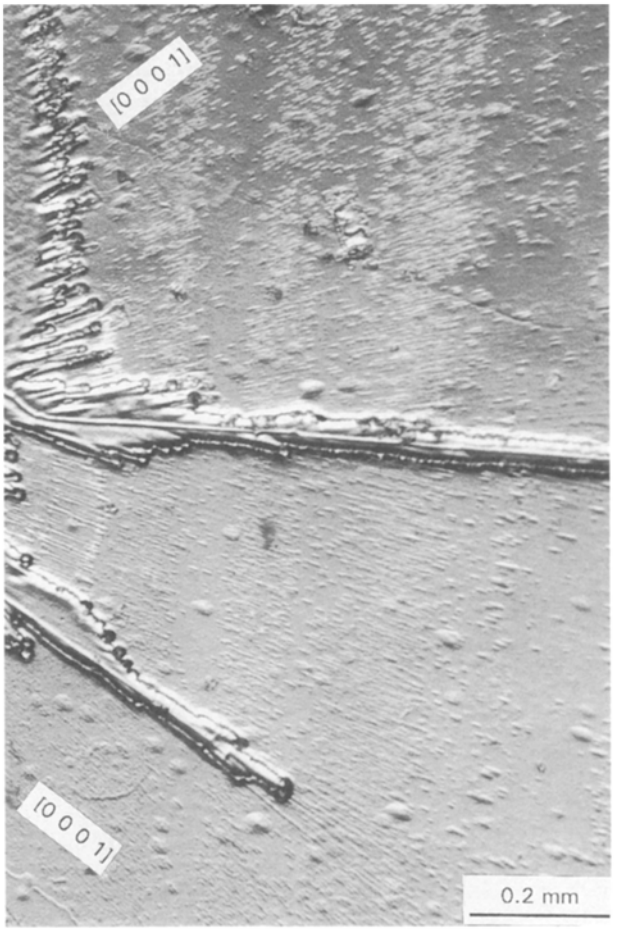

Figure 10 Replicated surface from an area in a curled tail of the specimen in Fig. 7b. Dislocation etch pits are elongated parallel to [0 0 0 1] (see [28]) and indicate a rotation of about 76° in the area shown. Two sub-grain boundaries are also displayed (represented by deeper grooves).

[29–31]. A variation in width of the shear zone from one run to the next is tentatively attributed to non-homogeneous distribution of dislocations prior to deformation. In one specimen, crystal slip was concentrated predominantly in very narrow zones parallel to the (0 0 0 1) lattice plane.

The geometry of the crystals deformed with this mode is comparable to that observed in the specimens compressed under *R* mode boundary conditions (compare Figs 6 and 12). However, the tilt walls do not occur in pairs. They are not as well defined and lattice curvature is less pronounced. This suggests the occurrence of a bending moment of a similar but somewhat less intense nature than that observed under full restriction, resulting from the constraint of only part of the crystal's volume.

5. Conclusion

Friction at the interface between a strongly anisotropic material element and the platens of a deformation apparatus, through which a compressive load is transmitted, is known to introduce a biaxial state of stress, represented by a plastic bending moment. This was observed in ice crystals machined into rectangular prisms and whose ends were mechanically constrained during creep tests at a high homologous temperature.

Relieving the constraints and minimizing friction at the ice–platen interface resulted in a variation of

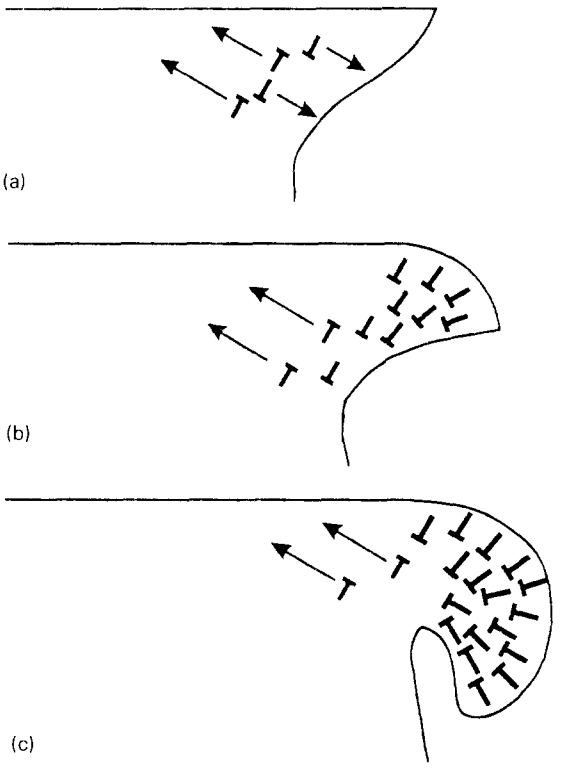

Figure 11 Model accounting for the development of a curled tail in opposite corners of the sample displayed in Fig. 7b.

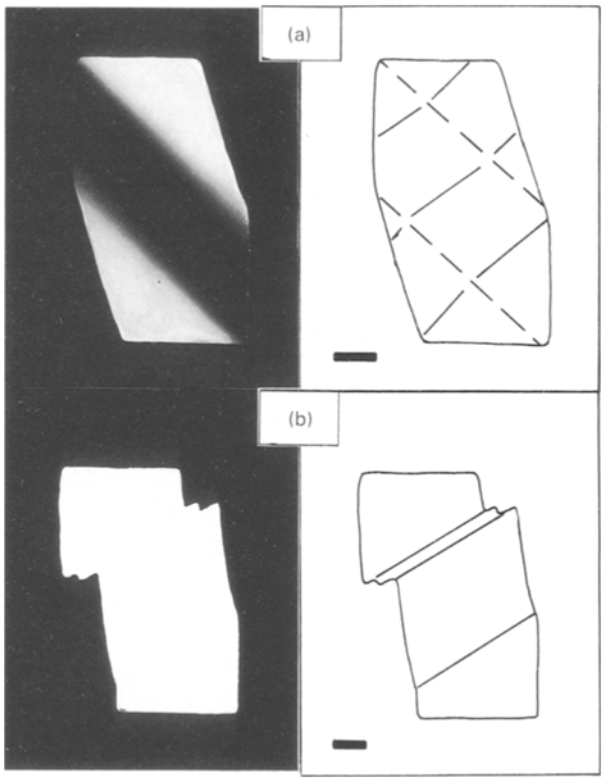

Figure 12 Sections of crystals deformed under *S* mode boundary conditions. (a) Axial strain is 9% with the (0 0 0 1) plane initially oriented at 45° to the load axis; (b) axial strain is 13% with the (0 0 0 1) plane initially oriented at 60° to the load axis. The thickness of the sections is 6 and 10 mm, respectively. Length of scale bars: 10 mm.

lattice orientation opposite to that obtained in crystals deformed in a fully constrained environment. This reversal is interpreted to originate from a bending moment of opposite sense, obtained from a variation in slip displacement in areas near the platens where segments of the lattice planes are shorter. Hence, unless careful adjustments of the load distribution are considered, it appears that non-homogeneous strain is inherent to ice crystals loaded under compression, whether or not friction is effective along the specimen–platen interface. This behaviour contrasts with that of other single-slip material deformed under similar conditions [32, 33]. It could be accounted for by higher dislocation glide velocity.

When widening at a specimen end was prevented, these shifted sideways with respect to each other as expected in an ideal case of single-slip plasticity. Slip was concentrated in the centre of the crystal into a shear zone of variable width. This represents a means of obtaining a simple shear regime under uniaxial compression.

Reference

1. R. W. K. HONEYCOMBE, "The plastic deformation of metals" (Edward Arnold, London, 1984).
2. C. N. REID, "Deformation geometry for materials scientists" (Pergamon Press, N.Y., 1973).
3. J.-P. A. IMMARIGEON and J. J. JONAS, *Acta Metall.* **19** (1971) 1053.
4. T. BRETHEAU and C. DOLIN, *J. Mater. Sci.* **13** (1978) 587.
5. J. P. POIRIER, "Creep of crystals" (Cambridge University Press, N.Y., 1985).
6. J. B. HESS and C. S. BARRETT, *J. Metals* **1** (1949) 599.
7. J. WASHBURN and E. R. PARKER, *ibid.* **4** (1952) 1076.
8. J. FRIEDEL, "Dislocations" (Pregamon Press, N.Y., 1967).
9. B. KAMB, in "Physics and chemistry of ice" (Royal Society of Canada, Ottawa) edited by E. Whalley, S. J. Jones and L. W. Gold (University of Toronto Press, Toronto, 1973) p. 28.
10. P. V. HOBBS, "Ice physics" (Clarendon Press, Oxford, 1974).
11. R. L. BROWN, in Proceedings of the 6th International Cold Regions Engineering Speciality Conference, edited by D. S. Sodhi (Cold Reg. Engineering, N.Y. American Society of Civil Eng. 1991) p. 483.
12. A. FUKUDA, T. HONDOH and A. HIGASHI, *J. Physique* **48** (suppl. to #3), Colloque C1 (1987) 163.
13. A. HIGASHI, "Lattice defects in ice crystals" (Hokkaïdo University Press, Sapporo, Japan, 1988).
14. J. W. GLEN and M. F. PERUTZ, *J. Glaciol.* **2** (1954) 397.
15. U. NAKAYA, in Symposium de Chamonix #47 (L'Association internationale d'hydrologie scientifique IASH, 1958) p. 229.
16. C. J. READINGS and J. T. BARTLETT, *J. Glaciol.* **7** (1968) 479.
17. P. DUVAL, M. F. ASHBY and I. ANDERMAN, *J. Phys. Chem.* **87** (1983) 4066.
18. S. AHMAD and R. W. WHITWORTH, *Phil. Mag. A* **57** (1988) 749.
19. W. B. KAMB, *J. Glaciol.* **30** (1961) 1097.
20. F. P. BLOSS, "An introduction to the methods of optical crystallography" (Holt Rinehart and Winston, Toronto, 1961).
21. P. BARRETTE, B. MICHEL and E. STANDER, *J. Cryst. Growth* **131** (1993) 153.
22. G. P. RIGSBY, *J. Glaciol.* **3** (1960) 589.
23. K. HIGUSHI, *ibid.* (1957) 131.
24. N. K. SINHA, *Phil. Mag.* **36** (1977) 1385.
25. N. K. SINHA, *J. Glaciol.* **21** (1978) 385.
26. A. H. COTTRELL, in "Progress in metal physics", edited by B. Chalmers (1949) p. 77.
27. R. W. CAHN and P. HAASEN, "Physical metallurgy" (North-Holland Physics Publishing, N.Y., 1983).
28. P. BARRETTE and N. K. SINHA, submitted to *J. Mater. Sci. Lett.*
29. G. P. RIGSBY, *J. Glaciol.* **3** (1958) 707.
30. S. STEINEMANN, *Beitrage zur Geologie der Schweiz (Hydrologie)* **10** (1958).
31. T. R. BUTKOVICH and J. K. LANDAUER, *SIPRE Res. Rep.* **56** (1959).
32. W. B. DURHAM and C. GOETZE, *J. Geophys. Res.* **82** (1977) 5737.
33. J. DODSWORTH, C. B. CARTER and D. L. KOHLSTEDT, in "Character of grain boundaries", edited by M. F. Yan and A. H. Heuer (American Ceramic Society, 1983) p. 73.

Received 17 January
and accepted 27 May 1994